Catalysis Science & Technology

COMMUNICATION

Continuous flow synthesis of Rh and Pd nanoparticles onto ion-exchange borate monoliths: application to selective catalytic hydrogenation of unsaturated carbonyl compounds under flow conditions[†]

Francesca Liguori and Pierluigi Barbaro*

Rhodium and palladium nanoparticles were generated within an unconventional polymeric borate monolith by a mild flow processes, and the resulting reactor used in the catalytic liquid-phase hydrogenation reaction of unsaturated carbonyl compounds under continuous flow, showing excellent conversions, durability and selectivity.

Molar fractions: x = 0.033; y = 0.651; z = 0.316

Fig. 1 Sketch of the composition (left) and optical camera image (right) of M@MonoBor (M = Pd, Rh).

Due to the considerable benefits in terms of purification, safety, waste emission, automation, energy consumption and space-time-yield productivity, heterogeneous catalysis under continuous flow is receiving increasing interest for use in selective chemical processes,[1] as these usually require stoichiometric reagents, protective groups, additives, expensive homogeneous catalysts or batch operations, causing severe economic and environmental problems.[2] In particular, *true monolithic* flow reactors[3] have shown to be extremely useful in the fine-chemicals synthesis because of the improved mass and heat transfer, lower pressure drop and uniform residence times distribution, compared to conventional packed-bed setups.[4] A limited number of inorganic[5] and polymeric[6] monoliths have been successfully used as support for selective chemical catalyst, including metal nanoparticles (MNP). Despite the simpler manufacture technology of polymeric monoliths,[7] issues have still to be solved concerning chemical stability, shrinking phenomena, limited porosity and catalyst deactivation, which adversely affect their performance as support materials.[8] Recently, we described the synthesis of PdNP immobilized onto a cation-exchange borate, macroporous resin monolith and their use in the catalytic semi-hydrogenation
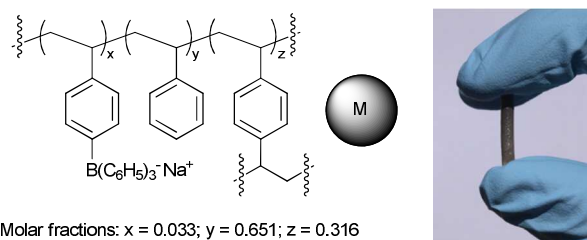
reaction of substituted alkynes under continuous flow.[9,10]

Herein we report on the mild, flow immobilization of RhNP onto MonoBor and the application of M@MonoBor (M = Pd, Rh, Fig. 1) to the selective, catalytic hydrogenation reaction of unsaturated carbonyl compounds under continuous flow conditions.

Following the approach we developed for the sustainable synthesis of ion-exchange resin-supported MNP,[11,12] which avoids use of toxic reagents, harsh conditions or sophisticated equipments,[13] *RhNP were generated in one-pot within MonoBor* by flowing a solution of $[Rh(NBD)_2]BF_4$ through a preformed monolith encased in a commercial glass column (3.0 i.d. x 25 mm length, 3 h @ 0.5 ml min^{-1}, rt,), followed by reduction under a stream of H_2 (1.5 bar, 2 ml min^{-1}, 3 h, rt). The as-prepared grey monolith Rh@MonoBor (0.82% w/w Rh loading, ICP-OES) was directly used in subsequent hydrogenation reactions under continuous flow, with no need of further treatments. TEM analysis revealed the presence of embedded RhNP of 3.9 ± 1.0 nm diameter (Fig. 2),[14] while EDS measurements showed the uniform radial and longitudinal distribution of the metal within the support, as illustrated in Fig. 3 in which carbon, sodium and Rh X-ray maps are reported for comparison. To the best of our knowledge this is *the first example of monolith-embedded RhNP*.[15,16]

Istituto di Chimica dei Composti Organo Metallici (ICCOM), Consiglio Nazionale delle Ricerche (CNR), Via Madonna del Piano 10, 50019 Sesto Fiorentino, Firenze, Italy
E-mail: pierluigi.barbaro@iccom.cnr.it
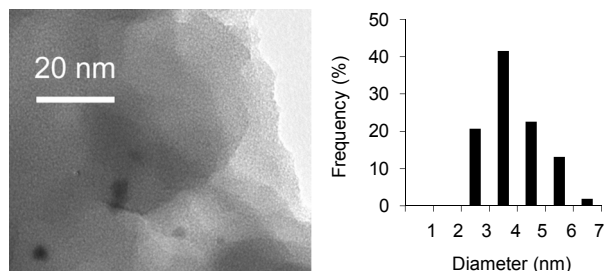
Fig. 2 Representative TEM image (right) and RhNPs size distribution (left) of Rr@MonoBor catalyst.

Fig. 3 From the left: EDS carbon (C Kα1), sodium (Na Kα1) and Rh (Rh Lα1) X-ray emission maps and ESEM image (secondary electrons) of a quadrant of a radial section of Rh@MonoBor monolith (25 keV, 70 magnifications).

The hydrogenation reaction of cyclohexene (**1**) was first used to evaluate the activity and the resistance of the novel Rh@MonoBor monolith catalyst, using an home-made reactor system allowing for concurrent flows of substrate solution and H_2 gas. Excellent conversions under very mild conditions (ca. 1 bar H_2 and rt, WSVH 4.2 - 6.8 h^{-1}) were observed, while the catalyst retained > 98% of its starting activity after 7 h time-on-stream (Fig. 4). A productivity of 9.9 mol_{1a} g_{Rh}^{-1} h^{-1}, corresponding to 1020 h^{-1} TOF and 1.1 kg l^{-1} h^{-1} STY, was estimated at 98% conversion on these basis (Table 1).[17] Conversion could be easily adjusted to 100 %, either by decreasing the solution flow rate (i.e. by increasing the residence time τ) or by increasing the hydrogen flow rate (i.e. by increasing the H_2 / substrate molar ratio), while selectivity to
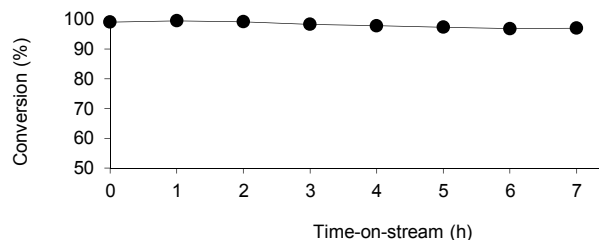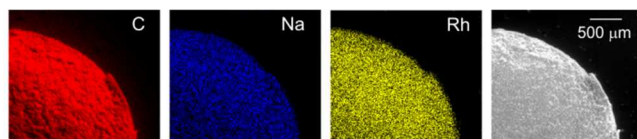

Fig. 4 Continuous flow hydrogenation of **1** over Rh@MonoBor catalyst (29 mg, 0.82% w/w Rh, 0.1 M methanol solution 0.40 ml min^{-1}, H_2 1.95 ml min^{-1}, 1.8 bar, rt, reactor volume 176 μl). Start time: attainment of steady state conditions (ca. 1 h).

cyclohexane (**1a**) was maintained above 99.9%. In no case rhodium leached in solution was detected by ICP-OES. The above results can be attributed to the strategic combination of strong metal anchoring on the non-coordinating support,[18,19] with the low pressure drop generated by the macroporous, rigid structure of the monolith.[9,10] Deactivation of ion-exchange resins-supported MNP catalysts was previously attributed to the loss of active species, to unfavourable interactions with the exchange groups, to the chemical degradation of the polymer under catalytic conditions and to the sintering of MNP,[11,20] that can be reasonably ruled out in our case.[21]
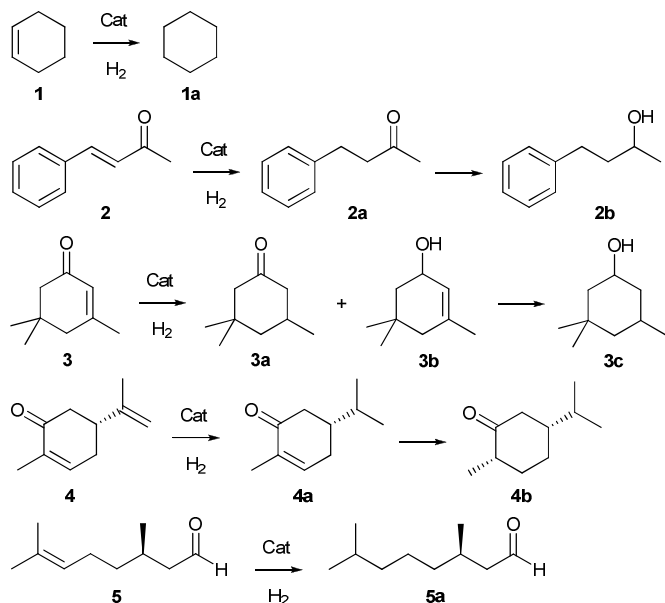
We then investigated the hydrogenation of the carbonyl compounds sketched in Scheme 1, under similar flow conditions, using both Rh@MonoBor and Pd@MonoBor catalysts. Various combination of H_2 and solution flow rates were used to evaluate the effect of the residence time and the H_2 / substrate ratio on the processes conversion and selectivity. As general trend, the catalysts showed high activity and selectivity to C=C bond hydrogenation, with slight selectivity decrease upon increasing conversion, as expected for similar systems.[22] Selected, best compromise results between conversion and selectivity are reported in Table 1.[17]

Thus, the hydrogenation of *trans*-4-phenyl-3-buten-2-one (**2**)

Table 1 Representative data for continuous flow hydrogenation reactions by M@MonoBor monolithic catalyst.

Substrate	Reaction conditions [a]						Conversion [e] (%)	Productivity [f] (mol_{prod} g_M^{-1} h^{-1})	Selectivity	
	Catalyst	Solution		H_2		H_2/Sub. ratio [d]			Prod.	(%) [g]
	M	Flow rate (ml min^{-1})	τ [b] (s)	Flow rate (ml min^{-1})	Pressure [c] (bar)					
1 cyclohexene	Rh	0.40	26	1.95	1.8	3.6	98.1 ± 1.0	9.9	**1a**	100.0
2 *trans*-4-phenyl-3-buten-2-one [h]	Rh	0.05	211	0.29	1.2	5.7	97.4 ± 0.9	0.6	**2a**	94.4
	Pd	0.05	211	0.25	1.4	5.7	100	0.8	**2a**	94.6
	Pd	0.10	106	0.47	1.5	5.7	99.5 ± 0.1	1.6	**2a**	96.0
3 isophorone [i]	Rh	0.20	53	0.90	1.4	8.2	91.4 ± 0.6	1.4	**3a**	96.3
	Pd	0.05	211	3.60	1.3	124	91.9 ± 1.0	0.4	**3a**	100.0
4 (*R*)-carvone [l]	Rh	0.18	59	0.43	1.2	11.9	92.0 ± 0.8	0.4	**4a**	77.6
	Rh	0.10	106	1.00	1.2	49	100	0.3	**4b**	85.7
	Pd	0.18	59	0.43	1.2	11.9	100	0.6	**4b**	67.1
5 (*R*)-citronellal [l]	Rh	0.03	352	3.50	1.3	594	57.0 ± 0.4	0.1	**5a**	100.0
	Pd	0.03	352	0.25	1.1	38	95.5 ± 0.9	0.1	**5a**	99.0

[a] Methanol solution 0.1 M, room temperature. Dry catalyst 29 mg, 0.82 % (w/w) Rh, 0.67 % (w/w) Pd. Reactor volume 176 μl. [b] τ = residence time. [c] Pressure measured at the reactor inlet. [d] Hydrogen to substrate molar ratio. [e] Data from GC analysis. Start time: attainment of steady state conditions, ca. 1h. Average value over 7 h time-on-stream. [f] Calculated from conversion average value. [g] For example, **2a** selectivity = **2a**/(**2a**+**2b**). [h] 0.05 M. [i] 0.03 M. [l] 0.01 M.

COMMUNICATION

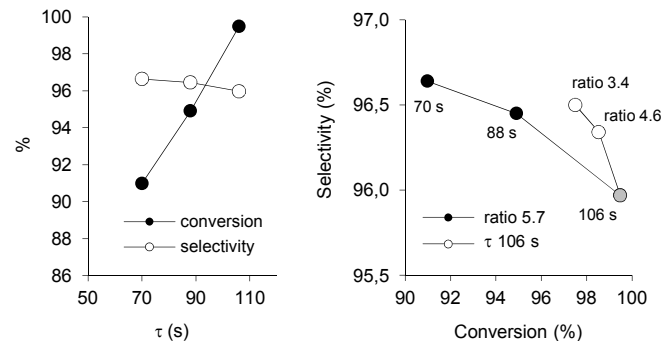**Scheme 1** Sketch of the substrates investigated and products detected.

Fig. 5 Continuous-flow hydrogenations of **2** over Pd@MonoBor catalyst (29 mg, 0.67% Pd w/w, rt, methanol, reactor volume 176 μl). Left: conversion and selectivity as a function of residence time τ (solution flow rate 0.05-0.15 ml min^{-1}) at fixed H$_2$:substrate ratio 5.7. Right: selectivity/conversion diagram at: ● fixed H$_2$/substrate ratio = 5.7 and residence time 70–106 s , ○ fixed residence time 106 s and H$_2$/substrate ratio range 3.4-5.7 (H$_2$ flow rate 0.30–0.47 ml min-1).
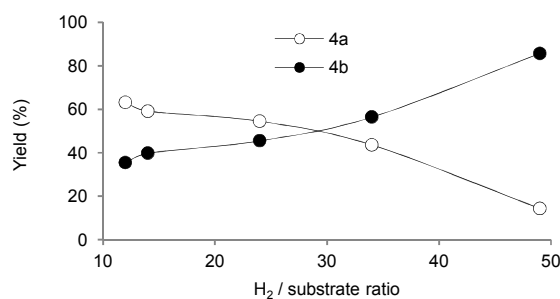

Fig. 6 Continuous-flow hydrogenation of **4** over Rh@MonoBor under fixed residence time 106 s and H$_2$/substrate ratio range 12-49 (H$_2$ flow rate 0.25–1.00 ml min^{-1}, catalyst 29 mg, 0.82% Rh w/w, rt, methanol, reactor volume 176 μl). Conversion above 98.5% in any case.

was accomplished with 94% selectivity to 4-phenyl-butan-2-one (**2a**) at 97% conversion using the Rh@MonoBor catalyst (τ 211 s, H$_2$/sub. ratio 5.7), corresponding to 0.6 mol g$_{Rh}^{-1}$ h^{-1} productivity. The Pd@MonoBor catalyst showed a better performance, providing similar selectivity at 100% conversion under the same flow conditions, and 96% selectivity at 99.5% conversion under optimized conditions (τ 106 s, H$_2$/sub. ratio 5.7), which corresponds to 1.6 mol g$_{Pd}^{-1}$ h^{-1} productivity. The relevant selectivity/conversion diagrams, obtained by varying the H$_2$ or the solution flow rates, are reported in Fig. 5. The only by-product detected was 4-phenyl-butan-2-ol (**2b**). This represents *the best result so far reported for the catalytic hydrogenation reaction of 2 under continuous flow*. The flow hydrogenation of **2** to **2a** was previously reported in 95% selectivity at 72% conversion using Pd@TiO$_2$ monolith catalyst.[5b] Results comparable with those reported in the present paper were only obtained under batch conditions using Pd@SiO$_2$ (70 °C, 1 bar H$_2$).[23]

Similarly, the important fine-chemical dihydroisophorone (**3a**)[24] was obtained by the hydrogenation of isophorone (**3**) over Rh@MonoBor in 96.3% selectivity at 91.4% conversion, with traces of **3b** and **3c** (τ 53 s). Pd@MonoBor was less active but more selective, requiring longer times (τ 211 s) to provide 100 % **3a** at the same conversion level. Previously reported flow hydrogenation of **3** using the comparable ion-exchange supported catalyst Pd@Dowex gave **3a** in 74.8% sel. at 84.6% conversion.[25,] Full conversion to **3a** was reported using 5%Pd@Deloxan in scCO$_2$ flow at 120 bar and 120 - 200 °C, however.[26] Poisoning of metal catalysts in the hydrogenation of **3** due to formation of oligomers has been described.[27]

The hydrogenation of (*R*)-(-)-carvone **4** over Rh@MonoBor was particularly intriguing, as it showed that careful tuning of the flow rates may drive the reaction to different partial hydrogenation products. Thus, use "soft" hydrogenation conditions (τ 59 s, H$_2$/sub

ratio 12) led to the preferential formation of carvotanacetone (**4a**) in 77.6% selectivity at 92% conversion, whereas adoption of overhydrogenation conditions (τ 106 s, H$_2$/sub. ratio 49) resulted in the production of *cis*-carvomenthone (**4b**) in > 90% selectivity at full conversion. Fig. 6 shows the yield dependence of **4a** and **4b** from the H$_2$ / substrate ratio in the range 12-49, at fixed τ 106 s. Interestingly, no C=O nor selective C=C ring bond hydrogenation products were whatsoever observed under the above conditions. Pd@MonoBor was less selective, invariably resulting in considerable amount (ca. 23%) of carvacrol dehydrogenation by-product, in addition to **4a** and **4b**.[28] Best selectivity results reported for the catalytic flow hydrogenation of **4** gave **4a** in 20% and **4b** in 80% yield, respectively, using Rh@Al$_2$O$_3$ in scCO$_2$.[29]

The tough substrate (*R*)-(+)-citronellal was quite resistant to hydrogenation, requiring long residence times (τ > 300 s) to achieve ca. 60% and 95% conversion over Rh and Pd@MonoBor, respectively. However, despite the large number of potentially obtainable products (due to competitive acetalisation, cyclization, isomerisation and hydrogenation reactions) the only product detected (*R*)-3,7-dimethyloctanal **5a** was due to partial hydrogenation, with unprecedented > 99% selectivity. Previous examples of catalytic flow hydrogenation of **5** resulted in mixtures of isopulegol and citronellol, or gave **5a** in ca. 80% sel. at ca. 60% conversion, with fast catalyst deactivation, however.[30]

Differences observed in the activity and selectivity of the Rh and Pd-catalyzed reactions are difficult to explain. Previous studies invoked a different adsorption mechanism on the metal surface.[29] MNP size may play a role, although the lack of direct connection between size and shape of RhNP and their catalytic activity was demonstrated.[31]

In conclusion, we have shown that borate monoliths may act as efficient support materials for Rh and PdNP catalysts under *very mild conditions, namely room temperature and 1-2 bar H_2, in both preparation and use.*[13,32] Compared to known systems, the catalysts offer reproducible, superior performances in the continuous flow, selective hydrogenation reactions of unsaturated carbonyl compounds, in terms of energy consumption, durability and selectivity at full conversion. Hydrogenation of challenging substrates derived from natural terpenoids was possible, to give important fine-chemicals, e.g. the polymer intermediate **3a**, the antimicrobial agent carvacrol,[33] the fungicide **4a**.[34]

Notes and references

1   For recent reviews see: (*a*) L. Vaccaro, D. Lanari, A. Marrocchi and G. Strappaveccia, *Green Chem*. 2014, **16**, 3680; (*b*) S.G. Newman and K.F. Jensen, *Green Chem*. 2013, **15**, 1456; (*c*) N. G. Anderson, *Org. Process Res. Dev*. 2012, **16**, 852; (*d*) J. Wegner, S. Ceylan and A. Kirschning, *Adv. Synth. Catal*. 2012, **354**, 17.

2   (*a*) R. A. Sheldon, I. Arends and U. Hanefeld, *Green Chemistry and Catalysis*, Wiley-VCH, Weinheim, 2007; (*b*) *Fine Chemicals Through Heterogeneous Catalysis*, Eds: R. A. Sheldon and H. van Bekkum, Wiley-VCH, Weinheim, 2001.

3   According to the definition given by IUPAC, a monoliths is "a shaped, fabricated intractable article with a homogeneous microstructure that does not exhibit any structural components distinguishable by optical microscopy" ("Definitions of terms relating to the structural and processing of sols, gels, networks and inorganic–organic hybrid materials", *IUPAC Recommendations*, 2007, pp. 1812). It shall not to be confused with conventional foams or honeycombs with millimetre size cavities, see: A. Cybulski and J. A. Moulijn, *Structured Catalysts and Reactors*, Marcel Dekker Ltd., New York, 2005, p 19.

4   A. Sachse, A. Galarneau, B. Coq and F. Fajula, *New J. Chem*. 2011, **35**, 259.

5   (*a*) A. Sachse, N. Linares, P. Barbaro, F. Fajula and A. Galarneau, *Dalton Trans*. 2013, **42**, 1378; (*b*) N. Linares, S. Hartmann, A. Galarneau and P. Barbaro, *ACS Catal*. 2012, **2**, 2194; (*c*) P. He, S. J. Haswell, P. D. I Fletcher, S. M. Kelly and A. Mansield, *Beilstein J. Org. Chem*. 2011, **7**, 1150.

6   For recent examples: (*a*) R. Bandaria and M. R. Buchmeiser, *Catal. Sci. Technol*. 2012, **2**, 220; (*b*) A. Gömann, J. A. Deverell, K. F. Munting, R. C. Jones, T. Rodemann, A. J. Canty, J. A. Smith and R. M. Guijt, *Tetrahedron* 2009, **65**, 1450; (*c*) N. Nikbin, M. Ladlow and S. V. Ley, *Org. Process Res. Dev*. 2007, **11**, 458.

7   F. Svec, J. Chromatogr. A 2010, **1217**, 902.

8   (*a*) U. Kunz, A. Kirschning, H. L. Wen, W. Solodenko, R. Cecilia, C. O. Kappe and T. Turek, *Catal. Today* 2005, **105**, 318; (*b*) S. Xie, R. W. Allington, J. M. Fréchet and F. Svec, in *Advances in Biochemical Engineering/Biotechnology*; Ed.: R. Freitag, Springer, London, 2002.

9   F. Liguori, S. Coiai, E. Passaglia and P. Barbaro, *Macromolecules* 2013, **46**, 5423.

10   F. Liguori and P. Barbaro, *J. Catal*. 2014, **311**, 212.

11   C. Moreno Marrodan, D. Berti, F. Liguori and P. Barbaro, *Catal. Sci. Technol*. 2012, **2**, 2279.

12   C. Moreno-Marrodan, F. Liguori, E. Mercadé and P. Barbaro, *unpublished work*.

13   J. A. Dahl, B. L. S. Maddux and J. E. Hutchison, *Chem. Rev*. 2007, **107**, 2228.

14   A surface / bulk metal atoms ratio of 28 % was estimated from TEM data, see: R. L. Johnston, *Atomic and Molecular Clusters*, Taylor & Francis, London, 2002. Chemisorption studies were hampered by the limited accessibility of gas reactants to monolith-embedded RhNP. XRD data were in line with those obtained by TEM.

15   While submitting the present paper, multimetallic alloy NP onto silsesquioxane monoliths were anticipated: N. Moitra, K. Kanamori, Y. H. Ikuhara, X. Gao, Y. Zhu, G. Hasegawa, K. Takeda, T. Shimada and K. Nakanishi, *J. Mater. Chem. A* 2014, **2**, 12535.

16   For a review on RhNP catalysts, see: A. Gual, C. Godard, S. Castillón and C. Claver, *Dalton Trans*. 2010, **39**, 11499.

17   See Supplementary Information for full experimental results table.

18   Due the dual effect of charged functional groups (electrostatic stabilization) and porosity (steric stabilization), see: B. Corain, K. Jeřábek, P. Centomo and P. Canton, *Angew. Chem., Int. Ed*. 2004, **43**, 959.

19   (*a*) I. Krossing and I. Raabe, *Angew. Chem. Int. Ed*. 2004, **43**, 2066; (*b*) R. Sablong, J. I. Van der Vlugt, R. Thomann, S. Mecking and D. Vogt, *Adv. Synth. Catal*. 2005, **347**, 633.

20   M. Kralik, B. Corain and M. Zecca, *Chem. Papers* 2000, **54**, 254.

21   No significant size change of RhNP was detected by TEM within the experimental errors after use in catalysis.

22   The selectivity observed can be justified by the greater affinity of Pd and Rh for C=C than for C=O bonds in aliphatic compounds: A. Roucoux, A. Nowicki and K. Philippot in *Nanoparticle and Catalysis*, Ed. D. Astruc, Wiely-VCH, Weinheim, 2007.

23   J. Toubiana, M. Chidambaram, A. Santo and Y. Sasson, *Adv. Synth. Catal*. 2008, **350**, 1230.

24   D. P. Cotrupe, W. E. Wellman and P. E. Burton, US 3446850, 1969.

25   C. Moreno-Marrodan, P. Barbaro, M. Catalano and A. Taurino, *Dalton Trans*. 2012, **41**, 12666.

26   M. G. Hitzler, F. R. Smail, S. K. Ross and M. Poliakoff, *Org. Process Res. Dev*. 1998, **2**, 137.

27   T. Sato, C. V. Rode, O. Sato and M. Shirai, *Appl. Catal B Environ*. 2004, **49**, 181.

28   C. I. Melo, R. Bogel-Łukasik and E. Bogel-Łukasik, *J. Supercrit. Fluid* 2012, **61**, 191.

29   C.I. Melo, R. Bogel-Łukasik, M. Gomes da Silva and E. Bogel-Łukasik, *Green Chem*. 2011, **13**, 2825.

30   (*a*) L. N. Protasova, E.V. Rebrov, H.E. Skelton, A.E.H. Wheatley and J.C. Schouten, *Appl. Catal. A Gen*. 2011, **399**, 12; (*b*) M. Burgener, R. Wirz, T. Mallat and A. Baiker, *J. Catal*. 2004, **228**, 152.

31   Y. Yuan, N. Yan and P. J. Dyson, *ACS Catal*. 2012, **2**, 1057.

32   J. M. Campelo, D. Luna, R. Luque, J. M. Marinas and A. A. Romero, *ChemSusChem* 2009, **2**, 18.

33   P. Rattanachaikunsopon and P. Phurnkhachorn, *J. Bioscience and Bioengineering* 2010, **110**, 614.

34   M. Znini, G. Cristofari, L. Majidi, J. Paolini, J.M. Desjobert and J. Costa, *LWT - Food Sci. Technol*. 2013, **54**, 564.

82x58mm (300 x 300 DPI)